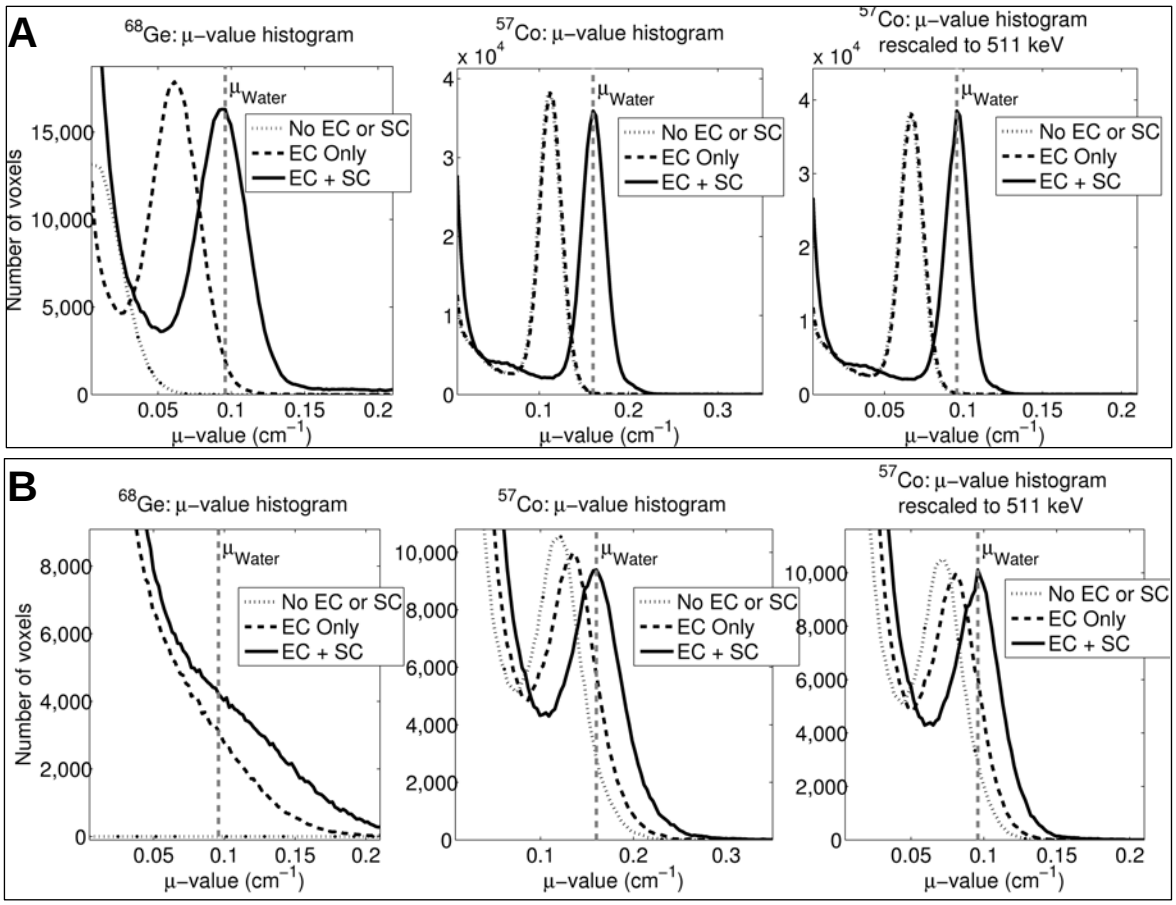


**Supplemental Figure 1.** Histograms of reconstructed linear attenuation coefficients (μ-value) corresponding to the $^{68}$Ge, $^{57}$Co and $^{57}$Co attenuation-maps which have been rescaled for 511 keV photons. The data shown in A is for the line source attached to a water cylinder while those in B are for post-injection rodent study. In each of the histograms, we also indicate the expected true linear attenuation coefficient for water or soft tissue ($\mu_{soft\text{-}tissue} \approx \mu_{Water}$=0.096 and 0.160 cm$^{-1}$ at 511 and 122 keV, respectively (18)). EC = emission-contamination correction; SC = scatter correction.

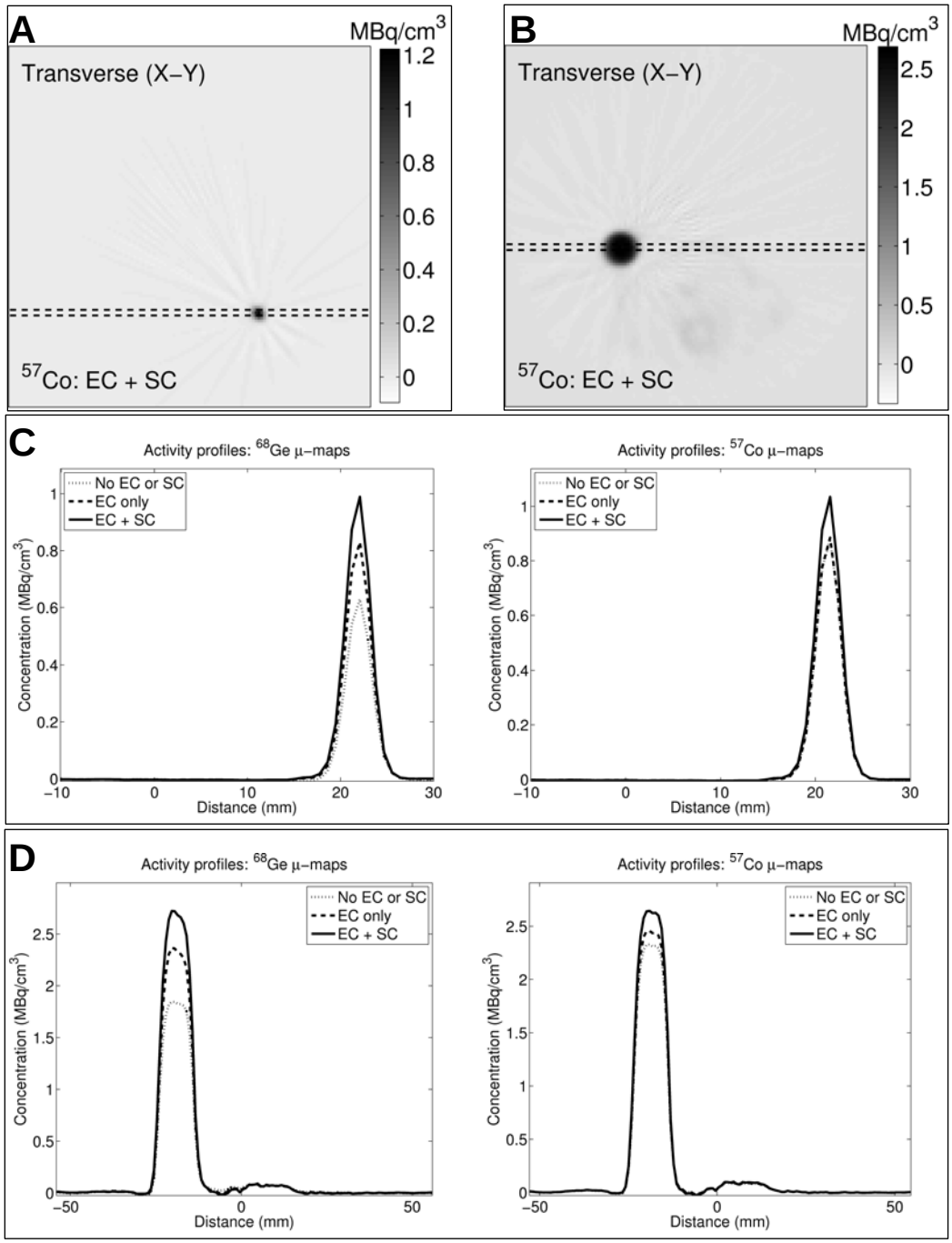


**Supplemental Figure 2.** Examples of transverse activity-concentration images (corresponding to the same slices shown in figures 3 and 4) for the cylinder (A) and rodent (B) studies. Note that the activity concentration within the rodent's body is much lower than that in the tumor and, therefore, the image of the rodent is more difficult to see in B. Images shown correspond to EC+SC attenuation-maps obtained using $^{57}$Co transmission data. The plots in C and D show profile data through each reconstructed activity image for the cylinder and rodent studies, respectively. The profiles were averaged over all data between the two dashed black lines shown in the images. EC = emission-contamination correction; SC = scatter correction.

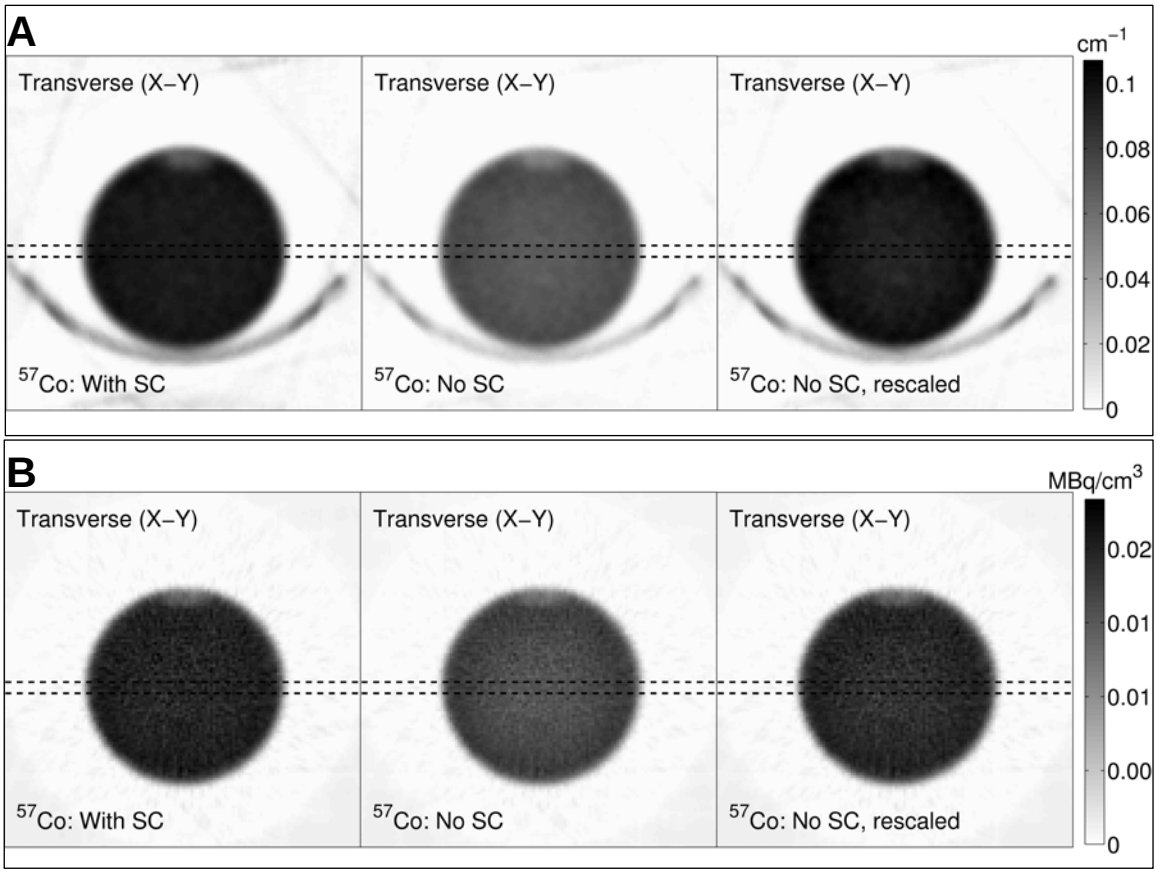


**Supplemental Figure 3.** Transverse attenuation images (A) and activity concentration images (B) for the 30 mm radius water cylinder using $^{57}$Co transmission data. Images were averaged over all axial planes to reduce noise and illustrate the systematic effects of scatter in the transmission data. Data shown corresponds to the scatter-corrected, uncorrected and the rescaled uncorrected attenuation-maps. SC = scatter correction.

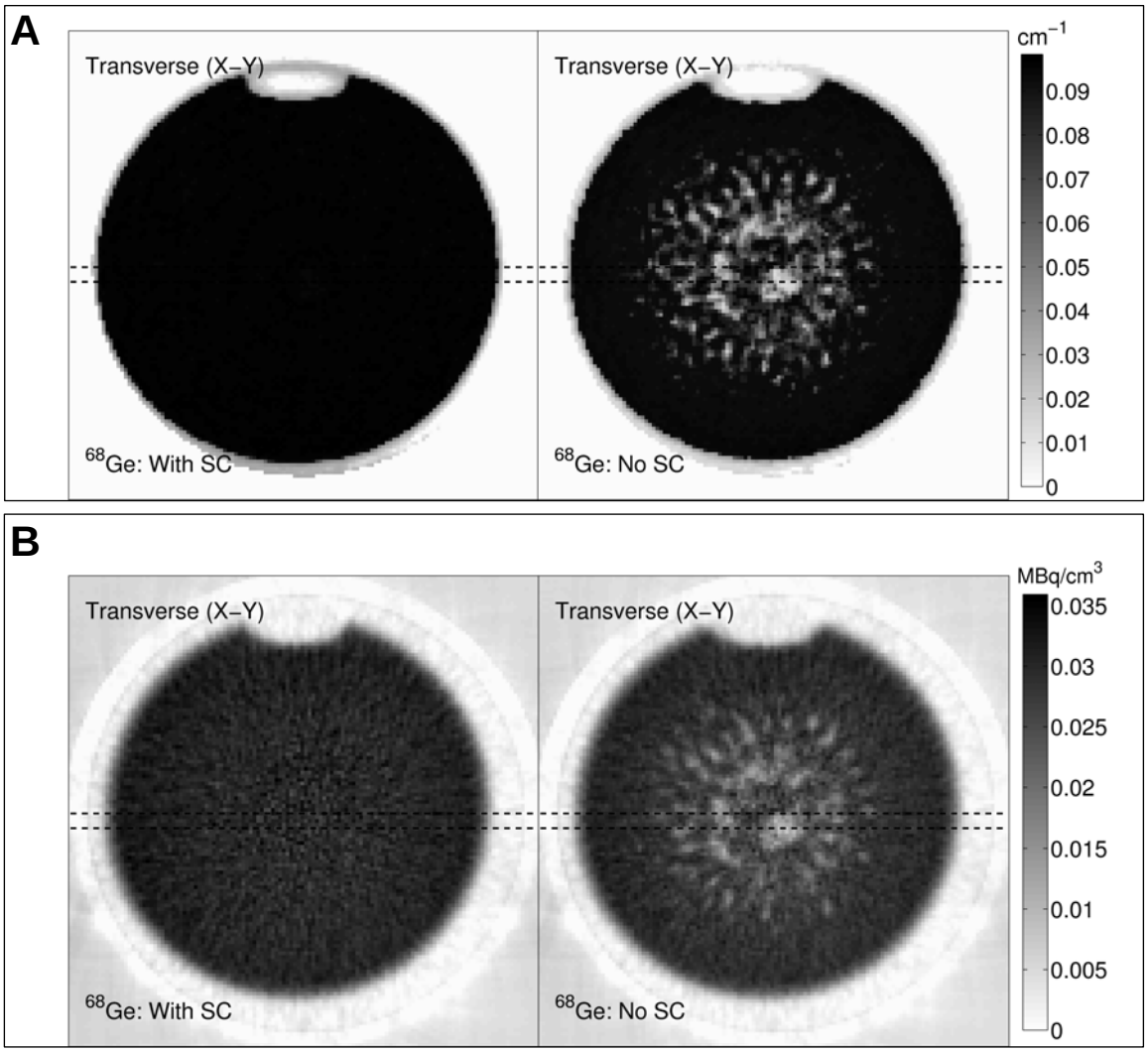


**Supplemental Figure 4.** Transverse attenuation images (A) and activity concentration images (B) for a central slice of the 45 mm radius water cylinder using $^{68}$Ge transmission data. Images were averaged over 10 axial planes to reduce noise in the emission data. The transmission data were reconstructed using MAPtr, the automated reconstruction-based segmentation method of Nuyts *et al.* (6), with and without transmission scatter corrections. SC = scatter correction.